JOURNAL OF OPTOELECTRONICS AND ADVANCED MATERIALS Vol. 10, No. 2, February 2008, p. 405 - 409

Controlled synthesis and photoluminescence of $Zn_3(PO_4)_2$: Eu^{3+} nanocrystal via hydrothermal process

JIANFENG GU, BINGYAN*
Department of Chemistry, Tongji University, Siping Road 1239, Shanghai 200092, China

In this paper, we have successfully prepared $Zn_3(PO_4)_2$: Eu^{3+} phosphors with regular morphologies via altering surface active agents. XRD, TEM and SEM have been used to investigate the synthesized powders, and the results show that all diffraction peaks of the product can be perfectly indexed by an orthorhombic phase with space group Pnma (62), the morphologies of the $Zn_3(PO_4)_2$: Eu^{3+} phosphors did not change greatly with the surface active agents altering, no mater using cetyltrimethylammonium bromide (CTAB) or PTG as surface active agent, we got $Zn_3(PO_4)_2$: Eu^{3+} nano-particles. We surmised that it may form the spherical micelles and then it played the role of the template and we got the products with the similar morphologies. Fourier transform infrared spectroscopy (FTIR) analysis was carried out to detect the products; ultraviolet – visible absorption spectra of the powder were recorded with a lambda 40 spectrometer. Finally, the photoluminescence of the products have been investigated, and found that Eu^{3+} ions in $Zn_3(PO_4)_2$ have the same symmetry, the magnetic dipole transition $^5D_0$-$^7F_2$ of Eu^{3+} ions is dominant, but the relative intensities are different.

(Received January 18, 2008; accepted February 7, 2008)

Keywords: Hydro-thermal synthesis, Zinc phosphate, Surface active reagents, Controlled microstructure, Photoluminescence

1. Introduction

In nature, $Zn_3(PO_4)_2 \cdot 4H_2O$ exists two forms: orthorhombic hopeite with orthorhombic structure and parahopeite with triclinic structure. Zinc phosphate has widespread application in coating, electric motors, transformers, and the automotive industry. It is also widely used as an alternative to the several nontoxic, anticorrosive pigments and so on [1].

Besides the application above, $Zn_3(PO_4)_2$ has also shown to be a host for rare earth or other ions to emit different luminescence. For example, $Zn_3(PO_4)_2$: Mn^{2+} was a typical and efficient phosphor for color television. Besides this, Eu^{3+} ions doped α- $Zn_3(PO_4)_2$ phosphor powders were prepared by using inorganic salts as raw materials and citric acid as coordinated reagent and the Eu^{3+} shows its characteristic red – orange (592 nm, $^5D_0$ – $^7F_1$) [2]. In the past few decades, nano-materials have attracted extraordinary research interest due to their fundamental significance for addressing some basic issue of the quantum confinement effect and space-confined transport phenomena, as well as their potential applications as advanced materials with collective properties [3]. The properties of nano-crystals depend not only on their chemical composition but also on their structure, phase, shape, size and size distribution. It is well-known that the macroscopic properties of phosphors, such as emission spectrum or luminous efficiency, are strongly dependent on the size, morphology, crystal type, and composition [4-9], so it is important to control the size, the morphology and microstructure. Therefore, there are lots of reports on the synthesis of nanometer and micro-scale phosphors with one - dimensional (1D) structures, such as wires or rods, tubes, coaxial cables, and belts or ribbons, and complex architectures based on 1D structure, such as branches, urchins, and networks [10-14]. It is reported particle size and morphology of the phosphors can be controlled by different methods, for instance, laser –assisted catalytic growth technique (LCG) [15], a vapor –liquid –solid (VLS) mechanism [16], and a solution – liquid- solid method (SLS) [17]. Several authors have also reported the synthesis of rare earth phosphate compounds via different methods: sol–gel, high temperature solid reaction and crystallization from boiling phosphoric acid solution or direct evaporation. The best solution to control the powder size and morphology is soft chemistry route and in particular the hydrothermal process, which are employed widely in the synthesis of rare earth ions doped inorganic compounds, such as yttrium vanadate, lanthanum fluoride, lanthanum phosphate, and yttrium oxide nano-particles [18-23].

It is well-known that reaction temperature, reaction time, pH, concentration and so on will influence the hydrothermal process, so it is possible to get $Zn_3(PO_4)_2$:Eu^{3+} phosphors with the different size and morphology by altering solvent and surface active agents. The phosphors with various microstructures have different growth anisotropy, and the morphologies may not be same. Surface active agent is another important factor to control the morphologies. In a chemical process, the surfactants are used templates and it is possible to directly obtain product with nanostructure, and they have been commonly

utilized as templates in the synthesis of nano-particles. Charged surfactants have also been used as stabilizers and templates for the growth of a variety of semiconductor and metallic nano-dots. Mixtures of cationic surfactants have recently been used as templates to prepare rod-shaped metallic and semiconductor nano-particles [24-26]. In most of the these studies ionic monomeric surfactants such as cetyltrimethylammonium bromide (CTAB) and sodium dodecylsulfate (SDS) have been frequently used as capping and micelle templates at high surfactant concentrations. With the concentration changing, the surfactant may form micelles, micro-emulsion, liquid-crystalline, vesicle systems and so on [27-28]. Therefore, it can be used as template to get the products wearing different morphologies. In this paper, we tried to alter the morphologies of $Zn_3(PO_4)_2$: Eu^{3+} phosphors by controlling the surfactants. We got the $Zn_3(PO_4)_2$: Eu^{3+} phosphors have no regular morphologies without any surfactant, but at the presence of the surfactants, the $Zn_3(PO_4)_2$: Eu^{3+} phosphors with regular shape appeared. It was well known that crystal growth and crystal morphology are governed by the degree of supersaturating, the diffusion of the reaction, the species to the surface of the crystals, the surface and interfacial energies, and the structure of the crystals. That is to say, the final morphology depends strongly on the extrinsic and intrinsic factors, the crystal structure, and the growth surroundings [29].

XRD, TEM and SEM have been used to investigate the synthesized powders, and the results show that all diffraction peaks of the product can be perfectly indexed by an orthorhombic phase with space group Pnma (62), the morphologies of the $Zn_3(PO_4)_2$: Eu^{3+} phosphors did not change greatly with the surface active agents altering, no mater using CTAB or PTG as surface active agent, we got $Zn_3(PO_4)_2$: Eu^{3+} nano-particles. We surmised that firstly, the surfactants have not formed micelles to serve as soft templates, the products had the same growth tendency and the shape were similar; secondly, it might form the spherical micelles and then it played the role of the template and we got the products with the similar morphologies. Finally, the photoluminescence of the products have been investigated, and found that Eu^{3+} ions in $Zn_3(PO_4)_2$ have the same symmetry, the magnetic dipole transition $^5D_0$-$^7F_2$ of Eu^{3+} ions is dominant, but the relative intensities are different.

2. Experiments

Preparation of $Zn_3(PO_4)_2$: Eu^{3+} phosphors

All samples were prepared by a simple hydrothermal method. The initiative materials were Eu_2O_3, $Zn(NO_3)_2$ and $NH_4H_2PO_4$. The Eu_2O_3 was added into concentrated nitric acid, and then it was heated until it was ropy, and $Eu(NO_3)_3$ was got. Then the $Zn_3(PO_4)_2$: Eu^{3+} phosphors were synthesized in the following: the $Eu(NO_3)_3$ we got above was mixed with appropriate amounts of $Zn(NO_3)_2$ in different solvent to form the emulsion, and then the surface active agent and $NH_4H_2PO_4$ were added to the mixture above, lately, the $NH_3.H_2O$ was added to adjust the PH value of the resultant solutions until the PH value was 9. Subsequently, the solution was poured into a Teflon lined stainless steel autoclave. Then the autoclave was sealed and maintained at 160 ℃ for 3 days, and then air cooled to room temperature. The resulting $Zn_3(PO_4)_2$: Eu^{3+}products were filtered, washed with distilled water and absolute alcohol to remove ions possibly remaining in the final products, and finally dried at 60 ℃ in air for further characterization.

3. Characterization

The X-ray powder diffraction (XRD) patterns of all samples were performed on a Bruke /D8-Advance with CuK a radiation (λ = 1.518 Å). The operation voltage and current were maintained at 40 kV and 40 mA, respectively. The scanning electronic microscopic images were obtained with Philips XL-30. Transmission electron microscopic images were obtained on a JEOL-2010 microscope with an accelerating voltage of 200 kV. Sample grids were prepared by ultrasonic powered samples in distilled water for about half an hour and then dripped the suspension onto a carbon- coated, holey film supported on a copper grid for TEM measurements. The excitation and emission spectra were recorded with Perkin-Elmer LS-55 model fluorometer equipped with a 150 W xenon lamp as the excitation source. Fourier transform infrared spectroscopy (FTIR) analysis was carried out using KBr disks in the region of 4000 – 400 cm^{-1} by using FTIR – Bruker – EQUINOX – 55 ambient conditions. Ultraviolet – visible absorption spectra of the powder were recorded with a lambda 40 spectrometer (Perkin – Elmer).

4. Results and discussion

We have examined the FTIR spectra of the hydrated $Zn_3(PO_4)_2$ samples with orthorhombic phase (shown in Fig. 4). Under such symmetry, three out of four fundamental vibration modes are IR active according to the selection rules. The active vibration modes in the range of 500 – 1100 cm^{-1} were ascribed to tetrahedral PO_4^{3-} anions and the patterns are basically consistent with the IR spectra of bulk monazite type $LnPO_4$. No pyrophosphate (P_2O_7 group, a typical band appearing at 1265 – 1267 cm^{-1}) impurity could be detected. Besides this, for the hydrated orthophosphates, there also exist the fundamental H_2O vibration modes. The corresponding band appeared at 1560 and 3400 cm^{-1}.

The morphologies of synthesized materials were ascertained using transmission electron dipole microscope (TEM), which were shown in Fig. 1. The images (A) and (B) in Fig. 1 showed that the $Zn_3(PO_4)_2$: Eu^{3+}phosphors using CTAB or PTG as surface active agent have the nanograin-like morphologies. From the results of X –ray

diffraction, we know that the $Zn_3(PO_4)_2$ phosphors (CTAB or PTG as surface active agent) wear the same orthorhombic phases, they may have the same growth tendency. It was also reported that in the hydrothermal process, crystal nucleation and crystal growth are determined by inherent crystal structure and the chemical potential in the precursor solution, which will affect the size and morphology of the crystalline powder. It is believed that the control in the morphologies are obviously related to the inherent structural characteristics of $Zn_3(PO_4)_2$ and external experimental conditions, such as reacting time, reaction temperature, surfactants, and solvents. So we can speculate that surface active agent is also a dominant factor to determine the final morphologies of the Zn_3 $(PO_4)_2$: Eu^{3+} phosphors. We surmised that: firstly, the surfactants have not formed micelles to serve as soft templates, the morphologies may be similar with the ones without any surface active agent; secondly, it may form the spherical micelles and then it played the role of the template and we got the products with the similar morphologies. The results showed that the $Zn_3(PO_4)_2$: Eu^{3+} phosphors have no regular morphologies, so it can be concluded that the surfactant has played as the template. The surfactant can retard the agglomeration of $Zn_3(PO_4)_2$: Eu^{3+} nano-particles, so the products have no agglomeration, and the particles are 20-30 nm in dimension.

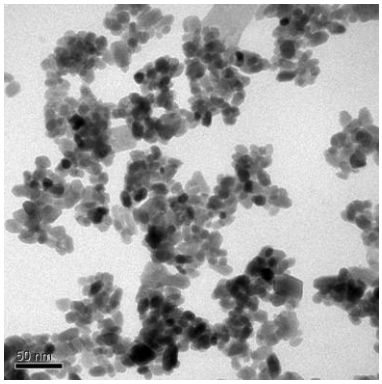

a

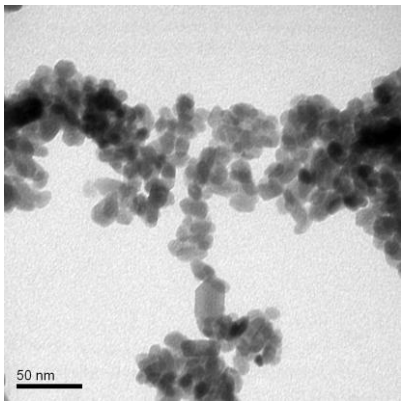

b

Fig. 1 TEM morphologies of prepared $Zn_3(PO_4)_2$: Eu^{3+}phosphors. (a) $Zn_3(PO_4)_2$: Eu^{3+} (CTAB); (b) $Zn_3(PO_4)_2$: Eu^{3+} (PTG).

The crystalline and purity of the products were examined by X –ray diffraction with Cu Ka radiation. XRD patterns of prepared $Zn_3(PO_4)_2$: Eu^{3+} is shown in Fig. 2. All diffraction peaks of the product can be perfectly indexed by an orthorhombic phase with space group Pnma (62), which were consistent with the literature data in the JCPDS file 33 – 1474 (orthorhombic, a = 10.61 nm, b = 18.31 nm, c = 5.030 nm). This indicates that under heating at 160 °C and starting at pH of 9, using CTAB or PTG as surface active agent, we can obtain the powders of the hydrated $Zn_3(PO_4)_2$. The $Zn_3(PO_4)_2$ phosphors prepared in the distilled water at the presence of CTAB or PTG wear the same structure, and they may have the same growth tendency and their morphologies are similar. The Fig. 1 (A) and (B) showed that the conjecture above was right, the $Zn_3(PO_4)_2$ phosphors using CTAB or PTG as surface active agent have the nanograin-like morphologies, and this result may also have relationship with the surfactant concentration, if the surfactant concentration exceed the critical concentration, the surface active agent (CTAB or PTG) will form spherical micelles and then it play the role of the template and we got the nano-particles.

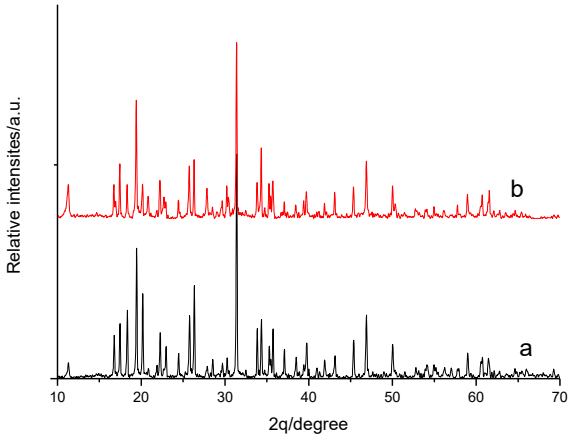

Fig. 2 XRD patterns of prepared $Zn_3(PO_4)_2$: Eu^{3+} phosphors. (a): (CTAB); (b): (PTG).

The excitation and emission spectra of Zn_3 $(PO_4)_2$: Eu^{3+} nano-particles are presented in Fig. 3 (A). All the excitation spectra of $Zn_3(PO_4)_2$: Eu^{3+} nano-particles are taken at an emission wavelength of 613 nm. It consists of a broad band in the shorter wavelength region from 200 to 280 nm, which are attributed to a charge transfer (CT) transition. This broad band took place by electron delocalization from an oxygen 2p orbital to an empty 4f orbital of europium ion. The position of the charge transfer

band (CTB) observed for $Zn_3(PO_4)_2$: Eu^{3+} show a little red shift by comparing to the bulk $Zn_3(PO_4)_2$: Eu^{3+} (261 nm) [30]. Besides, the sharp lines in the longer wavelength of 300 – 400 nm were observed in the spectra, corresponding to direct excitation of the Eu^{3+} ground state to higher levels of the 4f – manifold, and their assignments are marked in the figure according to the previous work [31]. At the same time, we have examined the absorption spectra of $Zn_3(PO_4)_2$: Eu^{3+} (shown in Fig.4 (B)), which involves several bands. The strong band peaked at 272 nm was ascribed to the absorption band of CTB (O – Eu) and a weaker band originating from the Eu^{3+} f – f transitions was also observed in the region of 300 – 400 nm, which was agreed with the excitation spectra.

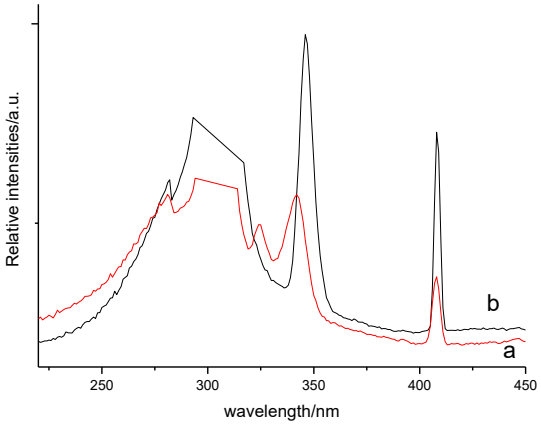

a

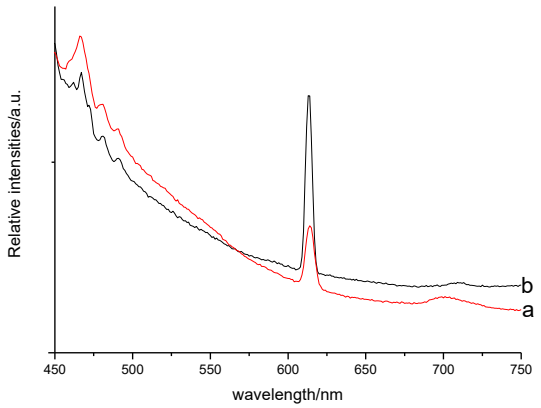

b

Fig. 3 Excitation (A) and emission (B) spectra of $Zn_3(PO_4)_2$:Eu^{3+} phosphors. (a): (PTG); (b): (CTAB)

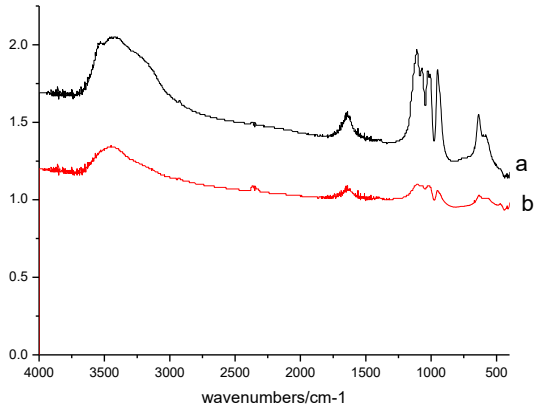

(a)

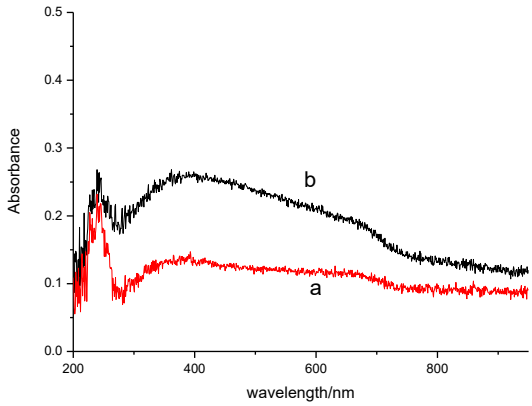

Fig. 4 (A) IR spectra of $Zn_3(PO_4)_2$: Eu^{3+} phosphors. (a): (PTG); (b): (CTAB) (B) Diffuse reflectance ultraviolet visible spectra of $Zn_3(PO_4)_2$: Eu^{3+} phosphors. (a): (CTAB); (b): (PTG).

The emission spectra of $Zn_3(PO_4)_2$: Eu^{3+} phosphors were monitored under the excitation wavelength at 408 nm, respectively. The emission spectra of Eu^{3+} activated phosphors have been involved in the following emission lines: $^5D_0$-$^7F_0$, $^5D_0$-$^7F_1$, $^5D_0$-$^7F_2$, $^5D_0$-$^7F_3$ and $^5D_0$-$^7F_4$, which are determined by transitions between its f – f electron energy levels. If the Eu^{3+} ions occupy an inversion symmetry site in the $Zn_3(PO_4)_2$ crystal lattice, the orange-red emission, magnetic transition $^5D_0$-$^7F_1$ (around 590 nm) is the dominant transition. On the contrary, the electric dipole transition $^5D_0$-$^7F_2$ (around 610-620 nm) is the dominant transitions [32-34]. According to the Judd – Ofelt theory, the magnetic dipole transition is permitted; however, the electric dipole transition is allowed only when the europium ion occupies a site without an inversion center and the intensity is significantly affected by the symmetry in local environments around Eu^{3+} ions [35]. As shown in the Fig. 3 (B), we can get the conclusion as the following: Eu^{3+} ions in the $Zn_3(PO_4)_2$ nano-particles

prepared at the presence of PTG or CTAB as surfactant have no inversion symmetry, so the electric dipole transition $^5D_0$-$^7F_2$ (613 nm) is the dominant transitions.

5. Conclusions

In summary, we have successfully synthesized $Zn_3(PO_4)_2$: Eu^{3+} phosphors with regular morphologies via altering surface active agents. XRD, TEM and SEM have been used to investigate the synthesized powders, and the results show that the morphologies of the $Zn_3(PO_4)_2$: Eu^{3+} phosphors did not change greatly with surface active agent altering, no mater using CTAB or PTG as surface active agent, we got $Zn_3(PO_4)_2$:Eu^{3+} nano-particles, which may be the result of concentration of the surfactants; only if the concentration exceeds the critical concentration, the surfactant can play the role of the template. We surmised that the both surfactants formed the spherical micelles and acted as templates, the nano-particles were also gotten. The emission spectra of $Zn_3(PO_4)_2$: Eu^{3+} phosphors have been investigated, and found that Eu^{3+} ions in the $Zn_3(PO_4)_2$ nano-particles prepared at the presence of PTG or CTAB as surfactant have no inversion symmetry, so the electric dipole transition $^5D_0$-$^7F_2$ (613 nm) is the dominant transitions.

References

[1] L. Herschke, V. Enkelmann, I. Lieberwirth, G. Wegner, Chem. Eur. J. **10**, 2795 (2004).
[2] W. Y. Shen, J. Lin, M.Yu, X. M. Han, J. Rare Earths **22**, 87 (2004).
[3] X.G. Peng, L. Manna, W.D. Yang, J. Wickham, E. Scher, A. Kadavanich, A.P. Alivisatos, Nature **404**, 57 (2000).
[4] J. Joo, T. Yu , Y .W. Kim, H. M. Park, F. Wu, J. Z. Zhang, T. Hyeon, J. Am. Chem. Soc. **125**, 6553 (2003).
[5] S. Lucas, E. Champion, D. Bregiroux, D. Bernache-Assollant, F. Audubert, J. Solid State Chem. **177**, 1302 (2004).
[6] X. C. Jiang, L. D. Aun, C. H. Yan, J. Phys. Chem. B **108**, 3387 (2004).
[7] D. Boyer, R. Mahiou, Chem. Mater. **16**, 2518 (2004).
[8] L. X. Yu, H. W. Song, S. Z. Lu, Z. X. Liu, L. M. Yang, X. K. Kong, J. Phys. Chem. B **108**, 16697 (2004).
[9] C. J. Jia, L. D. Sun, L. P. You, X. C. Jiang, F. Luo, Y. C. Pang, C. H. Yan, J. Phys. Chem. B **109**, 3284 (2005).
[10] L. Vayssieres, Adv. Mater. **15**, 464 (2003).
[11] J. Q. Hu, Q. Li, X. M. Meng, C. S. Lee, S. T. Lee, Chem. Mater **15**, 305 (2003).
[12] Z. W. Pan, Z. R. Dai, Z. L. Wang, Science **291**, 1947 (2001).
[13] G. Shen, Y. Bando, C. J. Lee, J. Phys. Chem. B **109**, 10578 (2005).
[14] C. X. Xu, X. W. Sun, B. J. Chen, Z. L. Dong, M. B. Yu, X. H. Zhang, S. J. Chua, Nanotechnology **16**, 70 (2005).
[15] F. Duan, C. M. Lieber, Adv. Mater. **12**, 298 (2000).
[16] V. F. Puntes, K. M. Krishnan, A. P. Alivosatos, Science **291**, 2115 (2001).
[17] T. J. Trentler, K. M. Hickman, S. C. Goel, A. M. Viano, P. C. Gibbons, W. E. Buhro, Science **270**, 1791 (1995).
[18] A. Huignard, T. Gacoin, J. P. Boilot, Chem. Mater. **12**, 1090 (2000).
[19] A. Huignard, V. Buissette, G. Laurent, T. Gacoin, J. P. Boilot, Chem. Mater. **14**, 2264 (2002).
[20] A. Huignard, V. Buissette, A. C. Franville, T. Gacoin, J. P. Boilot, J. Phys. Chem. B **107**, 6754 (2003).
[21] V. Buissette, A. Huignard, T. Gacoin, J. P. Boilot, P. Aschehoug, B. Viana, Surf. Sci. **444**, 532 (2003).
[22] K. Riwotzki, M. Haase, J. Phys. Chem. B **102**, 10129 (1998).
[23] J. W. Stouwdam, J. M. Veggel, Nano Lett. **2**, 733 (2002).
[24] J. Tanori, M.P. Pileni, Langmuir **13**, 639 (1997).
[25] Y. Ying, S.S. Chang, C.L. Lee, C.R.C. Wang, J. Phys. Chem. B **101**, 6661 (1997).
[26] C.C. Chen, C.Y. Chao, Z.H. Lang, Chem. Mater. **12**, 1516 (2000).
[27] J. H. Fendler, Chem. Rev. **87,** 877 (1987).
[28] Y. Li, J. Wan, Z. Gu**,** Mater. Sci. Eng. A **286**, 106 (2000).
[29] Q. Tang, W. Zhou, W. Zhang, S. Ou, K. Jiang, W. Yu, Y. T. Qian, Cryst. Growth Des. **5**, 147 (2005).
[30] W. Y.Shen, J. Lin, M.Yu, X. M.Han, J. Rare Earths **22**, 87 (2004).
[31] H. Meyssamy, K. Riwotzki, A. Kornowski, S. Naused, M. Haase, Adv. Mater. **11**, 840 (1999).
[32] H. H. Huang, B. Yan, Inorg. Chem. Commun. **7**, 717 (2004).
[33] Y. Q. Yu, S. H. Zhou, S. Y. Zhang, J. Alloys Compds. **84**, 351 (2003).
[34] P. S. Pizani, E. R. Leite, F. M. Pontes, E. C. Paris, J. H. Rangel, J. H. Lee, E. Longo, P. Delega, J. A. Varela, Appl. Phys. Lett. **77**, 824 (2000).
[35] J. Dexpert-Ghys, R. Mauricot, M. D. Faucher J. Lumin. **27**, 203 (1996).

*Corresponding author: byan@tongji.edu.cn